Model-based Analysis of Pulse Transit Time Characteristics During Obstructive Apnea

Arthur Ben-Tolila[1], Virginie Le Rolle[1], Jean-Louis Pépin[2], Alfredo I Hernández[1]

[1] Univ Rennes, Inserm, LTSI - UMR 1099, F-35000 Rennes, France
[2] Grenoble Alps University, HP2 laboratory, Inserm, U1042, Grenoble, F-38000, France

Abstract

The pulse transit time (PTT) is a non-invasive marker calculated as the time between the ECG R-wave and the pulse arrival at a peripheral vascular bed, which has been validated for apnea detection in sleep apnea syndrome (SAS). However, the mechanisms behind PTT behavior are complex and interrelated. In this work, a model-based approach is employed to investigate the modulations of PTT around obstructive apneas. PTT was synthesised from an integrated model of cardio-respiratory interactions, using a hemodynamic finger compartment, and a Morris sensitivity analysis was performed on model parameters for mean PTT and PTT oscillations. The most influent parameters were related to cardiac contractility, heart rate control, baroreflex, and CO_2 sensitivity. This work highlights the potential uses of PTT and paves the way towards patient-specific modeling during obstructive apneas.

1. Introduction

Sleep apnea syndrome (SAS) is defined by breathing cessation or reduction during sleep, which causes intermittent hypoxia, sleep fragmentation, and cardiovascular complications. The gold standard for diagnosis of SAS is performed through overnight polysomnography in a sleep center; however, there is a need for the development of accurate noninvasive diagnostic methods [1, 2].

The pulse transit time (PTT) is defined as the time from the R-wave on the ECG to the arrival of the pulse wave at a peripheral site measured using photoplethysmography (PPG). PTT has been shown to correlate with respiratory effort and has been validated for the detection of sleep apnea [2–6]. However, the interpretation of PTT remains difficult because of the complex interactions between several physiological mechanisms (nervous regulation, cardiac functions...).

In this context, computational modeling could be used to analyse the influence of cardiovascular and respiratory systems on PTT signals, in obstructive SAS, through the integration of physiological knowledge. Recently, our group has proposed a closed-loop, integrated model of cardio-respiratory interactions for the analysis of SAS in adults [7, 8]. The systemic circulation has been adapted to simulate PTT in [9]. In this work, the neural control was integrated and an obstructive apnea was simulated in order to provide physiological interpretations of PTT modulations during apnea. The simulation results were confronted with real data, and a parametric analysis of the model was performed to identify the most influent on PTT characteristics.

2. Methods

2.1. Database

The clinical database was obtained within the framework of the HYPNOS study [10]. Each patient in this study underwent one full-night polysomnograhy recording, and their respiratory events were annotated by the core laboratory. Among the 42 recordings, 11 were excluded from this study due to missing signals or annotations. The ECG and PPG signals in each recording were sampled at 1024 Hz and apneas were annotated with a precision of 1 second.

2.2. Apnea selection

For each recording in the database, annotated obstructive apneas were selected according to the following criteria: 1) minimum duration of 10 seconds and 2) a minimum separation between other apneas (central or obstructive) by at least 30 seconds, to limit interactions between consecutive events. For each apnea, a segment, including ECG and PPG signals, was studied from 30 seconds before the onset of the apnea to 30 seconds after the end of the apnea. Segments with cardiac arrythmias, or heavy artifacts on the ECG and/or PPG signals, were removed from the selection.

2.3. PTT calculation and processing

RR series extraction: From the ECG of each patient,

R-wave occurrence times t_b^R were extracted using the detector developed by Doyen et al. [11] for each beat b, and a statistical filter reimplemented in Python from Kaplan's HRV Toolbox [12] was applied on the R to R interval durations $(t_b^R - t_{b-1}^R)$ to remove incoherent beats.

PPG processing: The PPG was low pass-filtered, at a cut-off frequency of 8 Hz, using a 4th-order Butterworth filter, applied in both forward and backward directions to remove phase distortion. Then, the pulse arrival times t_b^P corresponding to each beat were determined using the intersecting tangents method [13] on PPG signals.

PTT processing: PTT samples were calculated as $PTT_b = t_b^P - t_b^R$, and placed at t_b^P. Two statistical filters were used to exclude outlier samples: one was applied on the (PTT_b) series, and the other on the series of inter-beat intervals $(t_b^P - t_{b-1}^P)$. The obtained (PTT_b) series was resampled at 1024 Hz to match the sampling frequency of the clinical and synthetic signals, and moving-average filtered with a 0.7s sliding window, resulting in signal $PTT_f(t)$.

PTT oscillations: ΔPTT was defined to quantify the amplitude of PTT_f oscillations due to thoracic pressure changes induced by respiration [2, 4]. A local minima $(t_j^m)_j$ and maxima $(t_j^M)_j$ detection was applied on PTT_f to obtain $\Delta PTT_j = PTT_f(t_j^M) - PTT_f(t_j^m)$, where $t_j^M < t_j^m$. The ΔPTT_j samples were placed at t_j^m, then resampled at 1024 Hz and moving-average filtered at 2 seconds to obtain $\Delta PTT_f(t)$.

Feature extraction: Finally, features were extracted from the PTT_f and ΔPTT_f signals : mean, standard deviation, and (max-min) amplitude. Three time periods were considered: 1) a 30-second window before the apnea, 2) during the apnea, and 3) a 30-second window after.

2.4. Model description

The proposed cardio-respiratory model (Fig. 1) is based on a previous model of our group [8, 9] and includes four major parts : i) the respiratory system, ii) the cardiovascular system, iii) the gas exchange system, and iv) the neural control system.

i) Respiratory system: The respiratory model [8, 14] is composed of the pleural cavity, the chest wall, the respiratory muscles, the airways (upper, intermediate and lower), and the alveolar compartment. A 20-second long obstructive apnea was modeled by simulating the collapse of the upper airway, by setting its resistance to 100000 $cmH_2O \cdot s \cdot l^{-1}$ at end-expiration.

ii) Cardiovascular system: The cardiovascular model includes the cardiac cavities, the systemic and pulmonary circulations (Fig. 2). The cardiac electrical system is modeled by a cellular automaton network. The atrial and the ventricular automaton trigger the mechanical activation of their respective cardiac cavities [8]. The maximal elastance of the atria and ventricles, and the venous unstressed volumes, are regulated by the baroreflex; the systemic and finger capillary resistances by the baroreflex and the peripheral chemoreflex. Each compartment of systemic and pulmonary circulations is associated with an unstressed volume V_u, an elastance E, a pressure P and volume V, where $P = E(V - V_u)$. Compartments are separated by resistances R, and inductances L in the case of the extrathoracic arteries and the finger arterial compartment. A finger compartment is defined in parallel to the systemic peripheral vessels compartment.

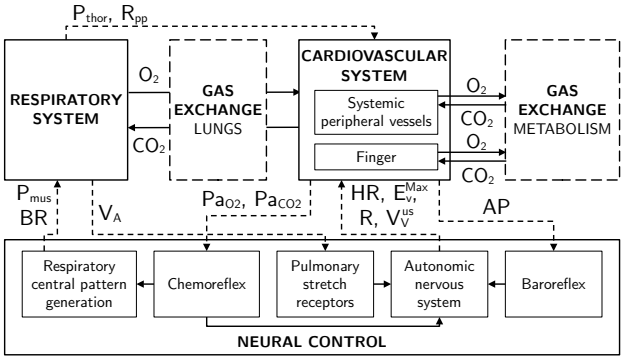

Figure 1: Diagram of the cardio-respiratory model, with arrows highlighting interactions between submodels. P_{thor}: thoracic pressure, R_{pp}: resistance of pulmonary capillaries, P_{mus}: respiratory muscles pressure, BR: breathing rate, Pa: partial pressure, HR: heart rate, E_v^{Max}: ventricular elastance, R: systemic resistance, V_V^{us}: venous unstressed volume, AP: arterial pressure.

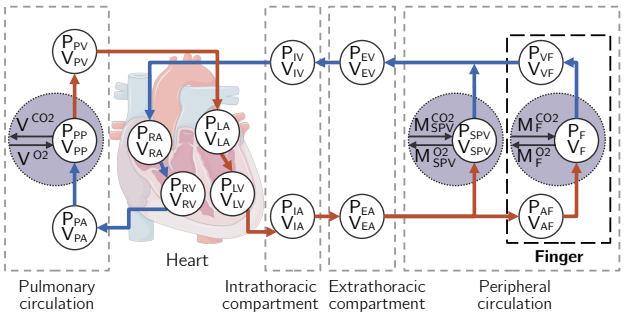

Figure 2: Diagram of the circulatory model and its compartments, each having a pressure (P) and volume (V). Indices: LA, LV: left atrium and ventricle, IA, IV: intrathoracic arteries and veins, EA, EV: extrathoracic arteries and veins, SPV: systemic peripheral vessels, AF, F, VF: finger artery, capillaries and vein.

iii) Gas exchange and transport: The *lung gas exchange* submodel [15] takes the O_2 and CO_2 fractions of inspired air as input, and outputs arterial gas concentrations, which are then transported into the systemic circulation with delays, using conservation of mass for blood flows. *Metabolic gas exchange* occurs in the systemic peripheral vessels compartment and in the finger compartment separately, with constant rates.

iv) Neural control: The neural control is separated into the chemoreflex [15] and baroreflex [16]. The *cen-*

Table 1: Comparison of the values obtained on the selected apneas (mean ± standard deviation) and on the model.

		Before	During	After
Mean PTT_f (ms)	Database	255 ± 16	258 ± 16	253 ± 16
	Model	252	254	255
Mean ΔPTT_f (ms)	Database	15 ± 6	15 ± 7	15 ± 5
	Model	12	20	20

tral chemoreflex is influenced by the arterial CO_2 partial pressure Pa_{CO2} around a set-point value Pa^n_{CO2}; the *peripheral chemoreflex* reacts to Pa_{O2} and Pa_{CO2}. Both types of chemoreceptors modulate the breathing rate and the pressure of the respiratory muscles. The *baroreflex* includes sympathetic (s) and parasympathetic (v) control of heart rate and integrates the influence of lung volume through the *pulmonary stretch receptors*; and sympathetic branches for modulation of the ventricular elastances, systemic resistances, and venous unstressed volumes. Each of these branches takes P_b as input, which is the intrathoracic arterial pressure P_{IA} filtered through a first-order transfer function, and comprises a sigmoid normalization function followed by a delay, and a first-order filter.

v) Synthesised PPG: The simulated pressure signal in the finger capillary compartment, denoted P_F, was used as an analog to PPG to calculate the pulse arrivals t_b^P with the intersecting tangents method, as in [9]. The heart beat times t_b^R were determined using the activation times of the left ventricular (LV) cardiac cell of the model. Synthesised PTT signals were processed as described in section 2.3.

2.5. Sensitivity analysis: Morris's method

Morris's screening method [17] was used to identify the most influential model parameters on PTT and ΔPTT characteristics, based on the evaluation of the mean (μ_i^*) and standard deviation (σ_i) of elementary effects. The distance $D_i = \sqrt{(\mu_i^*)^2 + (\sigma_i)^2}$ was used to rank the importance of each parameter. The output functions are the features described in section 2.3. Parameters were studied in a range of ± 20% of their initial value, using a grid of $p = 26$ levels, over 300 iterations.

3. Results and discussion

3.1. Comparison of patient and simulation values

After apnea selection, 381 segments were selected for analysis, with a mean apnea duration of 18 ± 9 s. Table 1 compares the indicators calculated on the database and on the model with its initial parameters, in the period before, during and after the apnea. The values obtained with the model are in agreement with the patient data, as well as the literature [2, 4, 13].

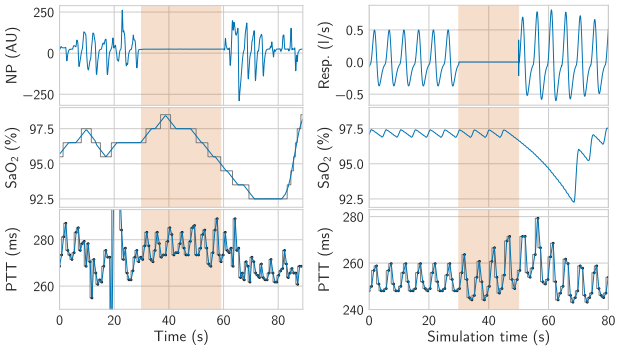

(a) Example patient (b) Simulation

Figure 3: Comparison of (a) a 21-s example apnea from the PASITHEA database, showing the uncalibrated nasal pressure (NP), the raw SaO_2, the PPG and the PTT, and (b) the simulation of a 20-s obstructive apnea, showing the upper airway flow, the tissue SaO_2, the finger capillary pressure P_F, and the PTT. The apnea is indicated by the solid red zone.

Fig. 3 shows an example obstructive apnea from the PASITHEA database, and the simulation results for a 20 second apnea. The model correctly reproduces the ΔPTT increase during the apnea, which is due to increased respiratory effort and blood pressure [2–4], and the post-apnea PTT drop, related to transient BP elevation and microarousal [6, 18].

3.2. Sensitivity analysis

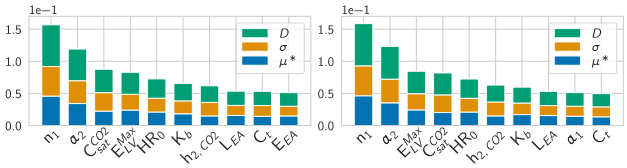

(a) Mean PTT_f during (b) Mean PTT_f after

Figure 4: Results of the Morris sensitivity analysis for the mean PTT_f (a) during and (b) after the obstructive apnea.

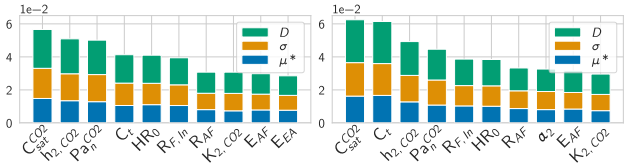

(a) Mean ΔPTT_f during (b) Mean ΔPTT_f after

Figure 5: Results of the Morris sensitivity analysis for the mean ΔPTT_f (a) during and (b) after the obstructive apnea.

Fig. 4 and 5 show the results of the Morris sensitivity analysis for the mean PTT_f and ΔPTT_f respectively, during and after the apnea. The 218 model parameters are sorted by Morris distance D_i, and only the 10 most influent are displayed for readability.

The **cardiac contractility**, associated with the maximal LV elastance E_{LV}^{Max}, directly affects the slope of the LV pressure P_{LV}, which modifies PTT. This is consistent with previous work [9] and the increased PTT observed in left

bundle branch block, where inotropy is usually reduced [19]. **Ventricular elastance parameters** (n_1 and α_2), that are associated with cardiac electro-mechanical function, also modify the LV pressure shape and PTT values.

Circulatory parameters affect blood pressures upstream and downstream from the finger compartment, modifying the shape of P_F. In accordance with previous findings [9] and the literature [13, 20], *extrathoracic (EA) and finger arterial (AF) parameters* increase the velocity of the pulse wave with stiffer arteries (larger E_{EA} and E_{AF}), lessened blood inertia (lower L_{EA}), and decreased vascular resistance (smaller R_{AF} and $R_{F,In}$). P_F is less damped and less respiration-modulated, yielding decreased PTT_f and ΔPTT_f.

The **baseline heart rate** HR_0 influences PTT_f and ΔPTT_f. Modifications of heart rate change the filling time of cardiac chambers, resulting in variations of the slope of P_{LV} through the Frank-Starling mechanism [20]. Moreover, **baroreceptors gain** K_b has also an overall influence on both the mean PTT_f and mean ΔPTT_f, by influencing both the inotropic and chronotropic control of the heart rate.

Pa_n^{CO2} is the set-point of the **central chemoreceptors** for the arterial CO_2 partial pressure, and C_t is involved in the afferent pathway to the **peripheral chemoreceptors**; C_{sat}^{CO2}, $h_{2,CO2}$, $\alpha_{2,CO2}$ and $K_{2,CO2}$ relate to the dissociation curve for the **pulmonary CO_2 concentration**. These parameters regulate the sensitivity of the model to CO_2 changes: a higher sensitivity translates to higher tidal volume and tissue SaO_2, therefore a lessened desaturation during the apnea, and increased respiratory modulation of P_F, leading to a higher ΔPTT_f. These findings are in accordance with the literature using PTT and its oscillations to distinguish obstructive and central apneas [2–5].

4. Conclusion

This work proposes a novel integrated model of cardio-respiratory interactions to synthesize the PTT signal in the context of SAS. Results highlight the most sensitive parameters related to cardiac contractility, baroreflex and chemoreflex regulation. Further work will focus on a more extensive sensitivity analysis and patient-specific identification of parameters to reproduce data observed from polysomnographic studies.

References

[1] Lévy P, et al. Obstructive sleep apnoea syndrome. Nature Reviews Disease Primers 2015;1(1):15015.

[2] Smith R, et al. Pulse transit time: an appraisal of potential clinical applications. Thorax 1999;54(5):452–457.

[3] Argod J, et al. Differentiating obstructive and central sleep respiratory events through pulse transit time. Am J Respir Crit Care Med 1998;158(6):1778–1783.

[4] Pitson D, et al. Use of pulse transit time as a measure of inspiratory effort in patients with obstructive sleep apnoea. Eur Respir J 1995;8(10):1669–1674.

[5] Pagani J, et al. Detection of central and obstructive sleep apnea in children using pulse transit time. In Computers in Cardiology, volume 29. 2002; 529–532.

[6] Kalantari E, et al. Evaluating changes in pulse transit time drop index in patients with obstructive sleep apnea before and during CPAP therapy. Clin Respir J 2022;16(9):611–617.

[7] Guerrero G, et al. Parametric analysis of an integrated model of cardio-respiratory interactions in adults in the context of obstructive sleep apnea. Ann Biomed Eng 2021; 49(12):3374–3387.

[8] Guerrero G, et al. Modeling patient-specific desaturation patterns in sleep apnea. IEEE Trans Biomed Eng 2022; 69(4):1502–1511.

[9] Ben-Tolila A, et al. Sensitivity analysis of a cardio-respiratory model for pulse transit time. In Computers in Cardiology, volume 50. 2023; 1–4.

[10] Hernández AI, et al. PASITHEA: An integrated monitoring and therapeutic system for sleep apnea syndromes based on adaptive kinesthetic stimulation. IRBM 2016;37(2):81–89.

[11] Doyen M, et al. Robust, real-time generic detector based on a multi-feature probabilistic method. PLoS ONE 2019; 14(10):e0223785.

[12] Kaplan D, Staffin P. Software for HRV, 1998.

[13] Finnegan E, et al. Pulse arrival time as a surrogate of blood pressure. Sci Rep 2021;11(1):22767.

[14] Le Rolle V, et al. Mathematical modeling of respiratory system mechanics in the newborn lamb. Acta Biotheor 2013; 61(1):91–107.

[15] Albanese A, et al. An integrated mathematical model of the human cardiopulmonary system: model development. Am J Physiol Heart Circ Physiol 2016;310(7):H899–H921.

[16] Le Rolle V, et al. Recursive identification of an arterial baroreflex model for the evaluation of cardiovascular autonomic modulation. Comput Biol Med 2015;66:287–294.

[17] Morris M. Factorial Sampling Plans for Preliminary Computational Experiments. Technometrics 1991;33(2):161–174.

[18] Pépin JL, et al. A critical review of peripheral arterial tone and pulse transit time as indirect diagnostic methods for detecting sleep disordered breathing and characterizing sleep structure. Curr Opin Pulm Med 2009;15(6):550.

[19] Villegas-Martinez M, et al. Pulse arrival time variation as a non-invasive marker of acute response to cardiac resynchronization therapy. EP Europace 2023;25(3):1183–1192.

[20] Hall JE, Hall ME. Guyton and Hall textbook of medical physiology. 14 edition. Elsevier, 2020.

Address for correspondence:

Virginie Le Rolle
Université de Rennes, LTSI, Rennes, 35042, France
virginie.lerolle@univ-rennes.fr